LUND UNIVERSITY

Modeling and Identification of Position and Temperature Dependent Friction Phenomena without Temperature Sensing

Bagge Carlson, Fredrik; Robertsson, Anders; Johansson, Rolf

Modeling and Identification of Position and Temperature Dependent Friction Phenomena without Temperature Sensing

Fredrik Bagge Carlson*   Anders Robertsson   Rolf Johansson

Abstract— **This paper investigates both positional dependence in systems with friction and the influence an increase in temperature has on the friction behavior. The positional dependence is modeled with a Radial Basis Function network and the temperature dependence is modeled as a first order system with the power loss due to friction as input, eliminating the need for temperature sensing. The proposed methods are evaluated in both simulations and experiments on two industrial robots with strong positional and temperature friction dependence.**

Index Terms— **Friction, System Identification, Radial Basis Function Network, Temperature Modeling**

I. INTRODUCTION

All mechanical systems with moving parts are subject to friction. The friction force is a product of interaction forces on an atomic level and is always resisting relative motion between two elements in contact. Due to the complex nature of the interaction forces, friction is usually modeled based on empirical observations. The simplest model of friction is the Coulomb model, Eq (1), which assumes a constant friction force acting in the reverse direction of motion

$$F_f = k_c \operatorname{sign}(v) \qquad (1)$$

where k_c is the Coulomb friction constant and v is the relative velocity between the interacting surfaces.

A slight extension to the Coulomb model includes also velocity dependent terms

$$F_f = k_v v + k_c \operatorname{sign}(v) \qquad (2)$$

where k_v is the viscous friction coefficient. The Coulomb model and the viscous model are illustrated in Fig. 2. If the friction is observed to vary with $\operatorname{sign}(v)$, the model (2) can be extended to

$$F_f = k_v v + k_c^+ \operatorname{sign}(v^+) + k_c^- \operatorname{sign}(v^-) \qquad (3)$$

where the sign operator is defined to be zero for $v = 0$ and $v^+ = \max(0, v)$ and $v^- = \min(0, v)$.
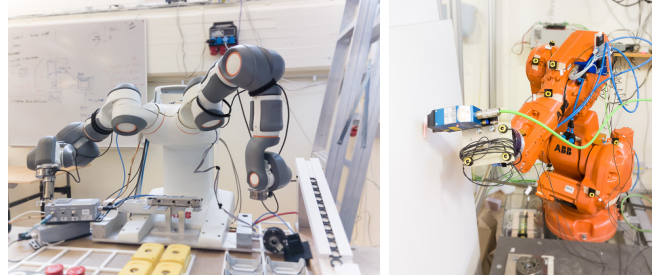
Fig. 1.   ABB YuMi and ABB IRB140 used for experimental verification of proposed models and identification procedures.
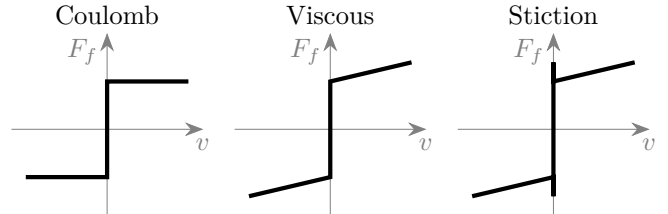
Fig. 2.   Illustrations of simple friction models.

It is commonly observed that the force needed to initiate movement from a resting position is higher than the force required to maintain a low velocity. This phenomenon, called stiction, is illustrated in Fig. 2. The friction for zero velocity and an external force F_e can be modeled as

$$F_f = \begin{cases} F_e & \text{if } v = 0 \text{ and } |F_e| < k_s \\ k_s \operatorname{sign} F_e & \text{if } v = 0 \text{ and } |F_e| \geq k_s \end{cases} \qquad (4)$$

where k_s is the stiction friction coefficient. An external force greater than the stiction force will, according to model (4), cause an instantaneous acceleration and a discontinuity in the friction force.

The models above suffice for many purposes but can not explain several commonly observed friction related phenomena, such as the Stribeck effect and dynamical behavior etc. [1]. To explain more complicated behaviour, dynamical models such as the Dahl model [2] and the LuGre model [3] have been proposed.

Most proposed friction models include velocity-dependent effects, but no position dependence. A dependence upon position is however often observed, and may stem from, for instance, imperfect assembly, irregularities in the contact surfaces or application of lubricant etc. [4]. Modeling of the position dependence is unfortunately nontrivial due to an often irregular relationship between the position and the friction force. Several authors have

however made efforts in the area. In [5] the author uses accurate friction measurements to implement a look-up table for the position dependence and in [6] the authors adaptively identify a sinusodial position dependence.

More recent endeavors include [7] where an Iterative Learning Control approach is used to learn a feedforward model including position dependent friction terms.

In [8], no significant positional dependence of the friction in a robot joint was found, however, a clear dependence upon the temperature of contact region was reported. To allow for temperature sensing, the grease in the gear box was replaced by an oil-based lubricant which allowed for temperature sensing in the oil flow circuit.

A standard approach in dealing with systems with varying parameters is recursive identification during normal operation [9]. Recursive identification of the models (1) and (2) could account for both position- and temperature dependence. Whereas straight forward in theory, it is often hard to perform in a robust manner in practical situations. Presence of external forces, accelerating motions etc. require either a break in the adaptation, or an accurate model of the additional dynamics. Many control programs, such as time-optimal programs, never exhibit zero acceleration, and thus no chance for parameter adaptation.

This paper suggests a model that incorporates positional friction dependence as well as a temperature dependent term. Since many industrially relevant systems lack temperature sensing in areas of importance for friction modeling, a sensor-less approach is proposed. Both models are used for identification of friction in the joint of an ABB YuMi robot, see Fig. 1, and special aspects of position dependence are verified on an ABB IRB140. The models and identification procedures are introduced in Sec. II and verification is performed in Sections III and IV. The paper is summarized in Sec. VI.

II. Models and Identification Procedures

This section first introduces a general identification procedure for linear models, based on the least-squares method, followed by the introduction of a model which allows for the friction to vary with position. Third, a model which accounts for temperature varying friction phenomena is introduced. Here, a sensor-less approach where the power loss due to friction is used as an input to a first order system, is adopted.

As the models are equally suited for friction due to linear and angular movements, the terms force and torque are here used interchangeably.

A. Least-Squares Identification

A standard model of the torques in a rigid-body dynamical system, such as industrial robots, is [10]

$$\tau = M(p)a + C(p,v)v + G(p) + F(v) \qquad (5)$$

where $a = \dot{v} = \ddot{p}$ is the acceleration, τ the control torque, M, C, G are matrices representing inertia-,

Coriolis-, centrifugal- and gravitational forces and F is a friction model. If a single joint at the time is operated, at constant velocity, Coriolis effects disappear [10] and

$$\left.\begin{array}{r} C(p,v) = 0 \\ a = 0 \end{array}\right\} \Rightarrow \tau = G(p) + F(v) \qquad (6)$$

To further simplify the presentation, it is assumed that $G(p) = 0$. This can easily be achieved by either aligning the axis of rotation with the gravitational vector such that gravitational forces vanish, by identifying and compensating for a gravity model[1] or, as in [8], performing a symmetric experiment with both positive and negative velocities and calculating the torque difference.

The simple models described in Sec. I are commonly identified with the well-known least-squares procedure [9], [11], [12]. For the model (2), this amounts to arranging data that satisfies Eq. (6) according to

$$y = \begin{bmatrix} \tau_1 \\ \vdots \\ \tau_N \end{bmatrix}, \; A = \begin{bmatrix} v_1 & \mathrm{sign}\,(v_1) \\ \vdots & \vdots \\ v_N & \mathrm{sign}\,(v_N) \end{bmatrix} \in \mathbb{R}^{N \times 2}, \; x = \begin{bmatrix} k_v \\ k_c \end{bmatrix} \tag{7}$$

and solving optimization problem (8) with solution (9).

$$x^* = \arg\min_{x} \left\| Ax - y \right\|_2 \qquad (8)$$

$$x^* = (A^{\mathsf{T}}A)^{-1}A^{\mathsf{T}}y \qquad (9)$$

B. Position Dependent Model

As mentioned in Sec. I, a positional, repeatable friction dependence is often observed in mechanical systems. This section extends the simple nominal models presented in Sec. I with position dependent terms, where the position dependence is modeled with a radial basis function network (RBFN)[2] [13].

Define the Gaussian RBF kernel κ and the kernel vector ϕ

$$\kappa(p, \mu, \sigma) = \exp\left(-\frac{(p-\mu)^2}{2\sigma^2}\right) \qquad (10)$$

$$\phi(p) : (p \in \mathcal{P}) \to \mathbb{R}^{1 \times K}$$
$$\phi(p) = \left[\kappa(p, \mu_1, \sigma), \cdots, \kappa(p, \mu_K, \sigma)\right] \qquad (11)$$

where $\mu_i \in \mathcal{P}, i = 1, ..., K$ is a set of K evenly spaced centers. For each input position $p \in \mathcal{P} \subseteq \mathbb{R}$, the kernel vector $\phi(p)$ will have activated (>0) entries for the kernels with centers close to p. The parameter σ in Eq. (10) determines the bandwidth of the RBFs. A large value of σ will result in a smooth estimate of the position dependence with low variance. Smaller values increase the variance but are able to capture finer detail. Refer

---

[1] For a single joint, this simply amounts to appending the regressor matrix A with $\begin{bmatrix} \sin(p) & \cos(p) \end{bmatrix}$

[2] Other common terms are Kernel Machines and RBF expansion.

to Fig. 3 for an illustration of RBFs. The kernel vector is appended the matrix A from Sec. II-A such that

$$A = \begin{bmatrix} v_1 & \text{sign}\,(v_1) & \phi(p_1) \\ \vdots & \vdots & \vdots \\ v_N & \text{sign}\,(v_N) & \phi(p_N) \end{bmatrix} \in \mathbb{R}^{N \times (2+K)}, \ x = \begin{bmatrix} k_v \\ k_c \\ k_\kappa \end{bmatrix} \tag{12}$$

where $k_\kappa \in \mathbb{R}^K$ denotes the parameters corresponding to the kernel vector entries. The number of RBFs to include and the bandwidth σ is usually chosen based on evidence maximization or cross validation [13].

The position dependent model can now be summarized as

$$F_f = F_n + k_\kappa \phi(p) \tag{13}$$

where F_n is one of the nominal models from Sec. I.

The above method is valid for position-varying Coulomb friction. It is conceivable that the position dependence is affected by the velocity, in which case the model (13) will produce a sub-optimal result. The RBF network can however be designed to cover the space $(\mathcal{P} \times \mathcal{V}) \subseteq \mathbb{R}^2$. The inclusion of velocity dependence comes at the cost of an increase in the number of parameters from K_p to $K_p K_v$, where K_p and K_v denote the number of basis function centers in the position and velocity input spaces respectively.

The expression for the RBF kernel will in this extended model assume the form

$$\kappa(x, \mu, \Sigma) = \exp\left(-\frac{1}{2}(x - \mu)^{\mathsf{T}} \Sigma^{-1} (x - \mu)\right) \tag{14}$$

where $x = \begin{bmatrix} p & v \end{bmatrix}^{\mathsf{T}} \in \mathcal{P} \times \mathcal{V}, \mu \in \mathcal{P} \times \mathcal{V}$ and Σ is the covariance matrix determining the bandwidth. The kernel vector will be

$$\phi(x) : \ (x \in \mathcal{P} \times \mathcal{V}) \to \mathbb{R}^{1 \times (K_p K_v)}$$
$$\phi(x) = \begin{bmatrix} \kappa(x, \mu_1, \Sigma), \cdots, \kappa(x, \mu_{K_p K_v}, \Sigma) \end{bmatrix} \tag{15}$$

This concept extends to higher dimensions, at the cost of an exponential growth in the number of model parameters.

1) Normalization: For some applications, it may be beneficial to normalize the kernel vector for each input point [14] such that

$$\bar{\phi}(x) = \left(\sum_{i=1}^{K_p K_v} \kappa(x, \mu_i, \Sigma)\right)^{-1} \phi(x) \tag{16}$$

One major difference between a standard RBF network and a normalized RBF network (NRBFN) is the behavior far (in terms of Mahalanobis distance) from the training data. The prediction of an RBFN will tend towards zero, whereas the prediction from an NRBFN keeps its value. Figure 3 shows two networks fit to the function $f(t) = 0.3t^2 - 0.5$ together with the basis functions used. The RBF tends towards zero both outside the data points and in the interval of missing data in the center. The NRBF on the other hand generalizes better and keeps its current
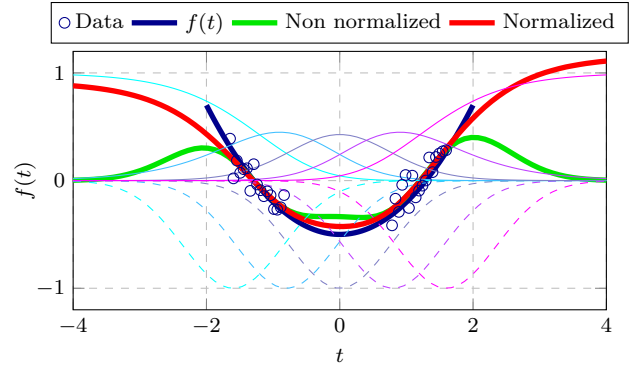

Fig. 3. RBF networks fit to noisy data from the function $f(t) = 0.3t^2 - 0.5$ using normalized (-) and non-normalized (- -) basis functions. Non-normalized basis functions are shown mirrored in the x-axis.

prediction trend outside the data. The performance of NRBF networks is studied in detail in [14].

C. Energy Dependent Model

Friction is often observed to vary with the temperature of the contact surfaces and lubricants involved [8]. Many systems of industrial relevance lack the sensors needed to measure the temperature of the contact regions, thus rendering temperature dependent models unusable.

The rise in temperature that occurs during operation is mostly due to friction losses. This section introduces a model which includes the generated energy, and estimates its influence on the friction.

A simple model for the temperature change in a system with temperature T, surrounding temperature T_s, and a power input W, is given by

$$\frac{dT(t)}{dt} = -k_s(T(t) - T_s) + k_W W(t) \tag{17}$$

for some constants k_s, k_W. After the variable change $\Delta T(t) = T(t) - T_s$, and transformation to the Laplace domain, the model (17) can be written

$$\Delta T(s) = \frac{k_W}{s + k_s} W(s) \tag{18}$$

where the power input generated by friction losses is equal to the friction force times the velocity

$$W(t) = |F_f(t)v(t)| \tag{19}$$

We are now ready to introduce the proposed model, which takes on the form

$$F_f = F_n + \text{sign}\,(v)E \tag{20}$$

$$E(s) = G(s)W(s) = \frac{\bar{k}_e}{1 + s\bar{\tau}_e} W(s) \tag{21}$$

where the friction force F_f has been divided into the nominal friction F_n and the signal E, corresponding to the influence of the thermal energy stored in the joint. The nominal model F_n can be chosen as any of the models previously introduced, including (13). The energy is assumed supplied by the instantaneous power due to friction, W, and is dissipating as a first order system with

time constant $\bar{\tau}_e$. A discrete representation is obtained after Zero-Order-Hold (ZOH) sampling [15] according to

$$E(z) = H(z)W(z) = \frac{k_e}{z - \tau_e}W(z) \qquad (22)$$

In the suggested model form (20) to (22), the transfer function $H(z)$ incorporates both the notion of energy being stored and dissipated, as well as the influence of the stored energy on the friction.

The proposed model suggests that the change in friction due to the temperature change occurs in the Coulomb friction. This assumption is always valid for the nominal model (1), and a reasonable approximation for the model (2) if $k_c \gg k_v v$ or if the system is both operated and identified in a small interval of velocities. If, however, the temperature change has a large effect on the viscous friction or on the position dependence, a 3D basis function expansion can be performed in the space $\mathcal{P} \times \mathcal{V} \times \mathcal{E}$, $E \in \mathcal{E}$. This general model can handle arbitrary nonlinear dependencies between position, velocity and estimated temperature. The energy signal E can then be estimated using a simple nominal model, and included in the kernel expansion for an extended model. Further discussion on this is held in Sec. V.

Denote by $\hat{\tau}_n$ the output of the nominal model F_n. Estimation of the signal E can now be done by rewriting Eq. (20) in two different ways

$$\hat{E} = (\tau - \hat{\tau}_n)\operatorname{sign}(v) \qquad (23)$$

$$F_n = \tau - \operatorname{sign}(v)\hat{E} \qquad (24)$$

The joint estimation of the parameters in the nominal model and $H(z)$ in Eq. (22) can be carried out in an Expectation-Maximization like fashion [13]. This amounts to iteratively finding an estimate $\hat{F}_n$ of the nominal model, using $\hat{F}_n$ to find an estimate $\hat{E}$ of E according to Eq. (23), using $\hat{E}$ to estimate $H(z)$ in Eq. (22) and, using $H(z)$, filter $\hat{E} = H(z)W$.

1) Initial Guess: For this scheme to work, an initial estimate of the paramters in $H(z)$ is needed. This can be easily obtained by observing the raw torque data from an experiment. Consider for example Fig. 4, where the system (20) and (21) has been simulated. The figure depicts the torque signal as well as the energy signal E. The envelope of the torque signal decays approximately as the signal E, which allows for easy estimation of the gain $\bar{k}_e$ and the time constant $\bar{\tau}_e$. The time constant $\bar{\tau}_e$ is determined by the time it takes for the signal to reach $(1 - e^{-1}) \approx 63\%$ of its final value. Since $G(s)$ is essentially a low-pass filter, the output $E = G(s)W$ will approximately reach $E_\infty = G(0)\mathbb{E}(W) = \bar{k}_e\mathbb{E}(W)$ if sent a stationary, stochastic input W with fast enough time constant ($\ll \bar{\tau}_e$). Here, $\mathbb{E}(\cdot)$ denotes the statistical expectation operator and E_∞ is the final value of the signal E. An initial estimate of the gain $\bar{k}_e$ can thus be obtained from the envelope of the torque signal as

$$\bar{k}_e \approx \frac{E_\infty}{\mathbb{E}(W)} \approx \frac{E_\infty}{\frac{1}{N}\sum_k W_k} \qquad (25)$$
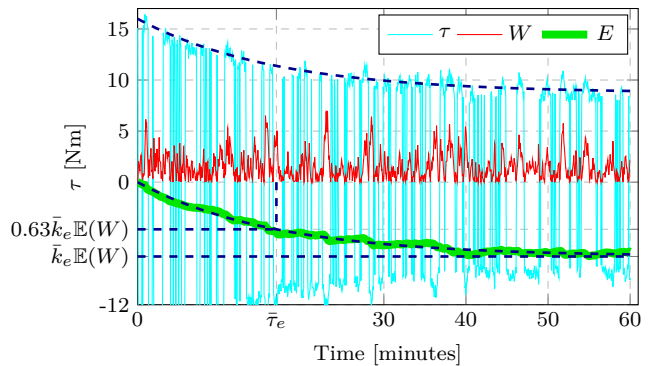

Fig. 4. A realization of simulated signals. The figure shows how the envelope of the applied torque approximately decays as the signal E. Dashed, blue lines are drawn to illustrate the determination of initial guesses for the time constant $\bar{\tau}_e$ and the gain $\bar{k}_e$.

Refer to Fig. 4 for an illustration, where dashed guides have been drawn to illustrate the initial guesses.

The discrete counterpart to $G(s)$ can be obtained by discretization with relevant sampling time [15].

2) Estimating the Model: An algorithm for the estimation of all parameters in Eqs. (20) to (22) is given in Algorithm 1. The estimation of $\hat{H}(z)$ in Eq. (22) can be done with e.g., the Output Error Method[3] [9] and the estimation of the nominal model is carried out using the LS procedure from Sec. II-A.

Algorithm 1 Estimation of the parameters and the signal E in the energy dependent friction model.

Require: Initial estimate $\hat{H}(z, k_e, \tau_e)$;
  repeat
    Calculate $\hat{E}$ according to Eq. (23);
    Update $\hat{H}(z)$ using Eq. (22);
    $\hat{E} \leftarrow \hat{H}(z)W$ ▷ Filter W through $\hat{H}(z)$;
    Update F_n according to (24) using Eq. (9);
  until Convergence

III. SIMULATIONS

To analyze the validity of the proposed technique for estimation of the energy dependent model, a simulation experiment was performed. The system described by Eqs. (20) and (21) was simulated to create 50 realizations of the relevant signals, and the proposed method was run for 50 iterations to identify the model parameters. The parameters used in the simulation are provided in Table I. Initial guesses were chosen at random from the uniform distributions $\hat{\bar{k}}_e \sim \mathcal{U}(0, 3\bar{k}_e)$ $\hat{\bar{\tau}}_e \sim \mathcal{U}(0, 3\bar{\tau})$.

Figure 5 shows that the estimated parameters converge rapidly to their true values, and Fig. 6 indicates that the Root Mean Square output Error (RMSE) converges to the level of the added measurement noise. Figure 6 further shows that the errors in the parameter estimates, as defined by Eq. (26), were typically below 5% of the

---

[3]E.g. Matlab System Identification Toolbox, command `oe()`

TABLE I

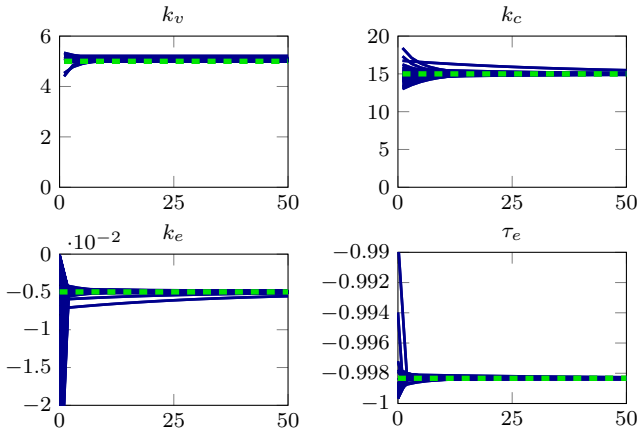| Parameter	k_v	k_c	k_e	τ_e	Measurement noise σ_τ	Sample time h	Duration	Iterations
Value	5	15	-3/-0.5	10/0.9983	0.5Nm	1s	3600s	50

Fig. 5. Estimated parameters during 50 simulations. The horizontal axis displays the iteration number and the vertical axis the current parameter value. True parameter values are indicated with green, dashed lines.
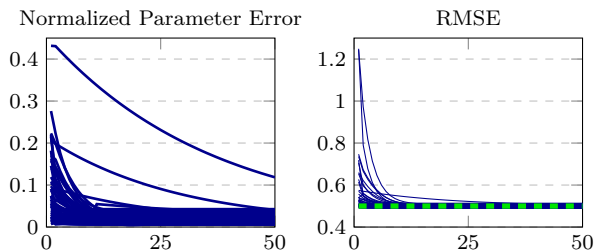

Fig. 6. Evolution of errors during the simulation experiment, the horizontal axis displays the iteration number. The left plot shows normalized norms of parameter errors, defined in Eq. (26), and the right plot shows the RMS output error using the estimated parameters. The standard deviation of the added measurement noise is shown with a green, dashed line.

parameter values.

$$\text{NPE} = \sqrt{\sum_{i=1}^{N_p} \left(\frac{\hat{x}_i - x_i}{|x_i|} \right)^2} \qquad (26)$$

IV. EXPERIMENTS

The proposed models and identification procedures were applied to data from an experiment with an ABB YuMi, and an ABB IRB140 industrial robot, see Fig. 1.

A. Procedure

For IRB140, the first joint was used. The rest of the arms were positioned so as to minimize the moment of inertia. For YuMi, joint four in one of the arms was positioned such that the influence of gravity vanished.

A program which moved the selected joint at piecewise constant velocities between the two joint limits was executed for approximately 20 min. Torque-, velocity-, and position data were sampled and filtered at 250 Hz and subsequently sub-sampled and stored at 20 Hz, resulting in 25 000 data points. Points approximately satisfying
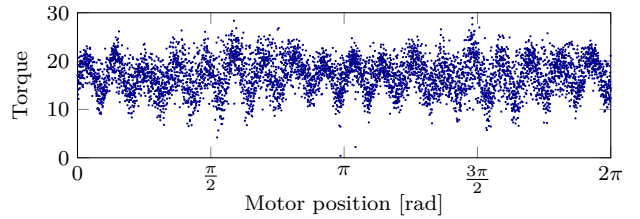

Fig. 7. Illustration of the torque dependence upon the motor position for the IRB140 robot.

Eq. (6) were selected for identification, resulting in a set of 16 000 data points.

1) Nominal Model: The viscous model (3) was fit using the ordinary LS procedure from Sec. II-A. This model was also used as the nominal model in the subsequent fitting of position model (13) and energy model (20) to (22).

2) Position Model: For the position dependent model, the number of basis functions and their bandwidth was determined using cross validation. A large value of σ has a strong regularizing effect and resulted in a model that generalized well outside the training data. The model was fit using normalized basis functions.

Due to the characteristics of the gear box in many industrial robots, there is a clear dependence not only on the arm position, but also on the motor position. Figure 7 shows the torque versus the motor position when the joint is operated at constant velocity. This is especially strong on the IRB140 and results are therefore illustrated for this robot. Both arm and motor positions are available through the simple relationship $p_{motor} = \text{mod}_{2\pi}(g \cdot p_{arm})$, where g denotes the gear ratio. This allows for basis function expansion also for the motor positions. To illustrate this, p_{motor} was expanded into $K_{p_m} K_v = 36 \times 6$ basis functions, corresponding to the periodicity observed in Fig. 7. The results for the model with motor position dependence are reported separately.

To reduce variance in the estimated kernel parameters, all position-dependent models were estimated using ridge regression [13], where a Gaussian prior was put on the kernel parameters. The strength of the prior was determined using cross validation. All basis function expansions were performed with normalized basis functions.

3) Energy Model: The energy dependent model was identified for YuMi using the procedure described in Algorithm 1. The initial guesses for $H(z)$ were $\bar{\tau}_e = 10$ min and $\bar{k}_e = -0.1$. The nominal model was chosen as the viscous friction model Eq. (3). Once the signal E was estimated, a kernel expansion in the space $\mathcal{P} \times \mathcal{V} \times \mathcal{E}$ with $40 \times 6 \times 3$ basis functions was performed to capture temperature dependent effects in both the Coulomb and viscous friction parameters.
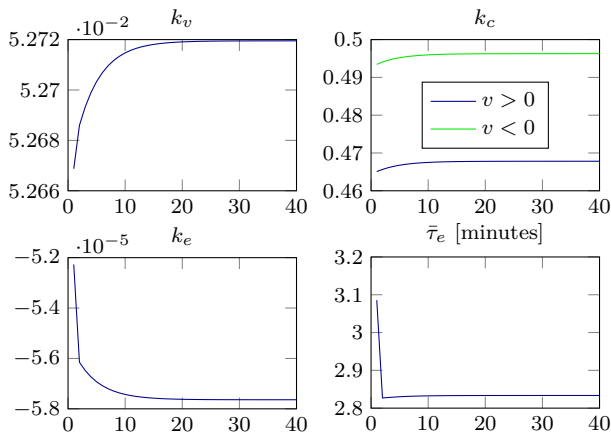
Fig. 8. Estimated parameters from experimental data. The horizontal axis displays the iteration number and the vertical axis the current parameter value.

TABLE II
PERFORMANCE INDICATORS FOR THE IDENTIFIED MODELS, YuMi.

	Nominal	Position	Position + Energy
Fit	86.968	93.193	96.674
FPE	3.63e-03	1.03e-03	2.65e-04
RMSE	6.03e-02	3.15e-02	1.54e-02
MAE	4.71e-02	2.36e-02	1.22e-02

B. Results

The convergence of the model parameters is shown in Fig. 8 and Fig. 9 illustrates how the models identified for YuMi fit the experimental data. The upper plot shows an early stage of the experiment when the joint is cold. At this stage, the model without the energy term underestimates the torque needed, whereas the energy model does a better job. The lower plot shows a later stage of the experiment where the mean torque level is significantly lower. Here, the model without energy term is instead slightly over estimating the friction torque. The observed behavior is expected, since the model without energy dependence will fit the average friction level during the entire experiment. The two models correspond well in the middle of the experiments (not shown). The nominal model (3), can not account for any of the positional effects and produces an overall, much worse fit. Different measures of model fit for the three models are presented in Table II and Fig. 11 (Fit (%), Final Prediction Error, Root Mean Square Error, Mean Absolute Error). For definitions, see e.g. [9].

For the IRB140, three models are compared. The nominal model Eq. (3), a model with a basis function expansion in the space $\mathcal{P}_{arm}$ and a model with an additional basis function expansion in the space $\mathcal{P}_{motor} \times \mathcal{V}$. The resulting model fits are shown in Fig. 10. What may seem like random measurement noise in the torque signal is in fact predictable using a relatively small set of parameters. Figure 12 illustrates that the large dependence of the torque on the motor position results in large errors. The inclusion of a basis function expansion of the motor position in the model reduces the error significantly.
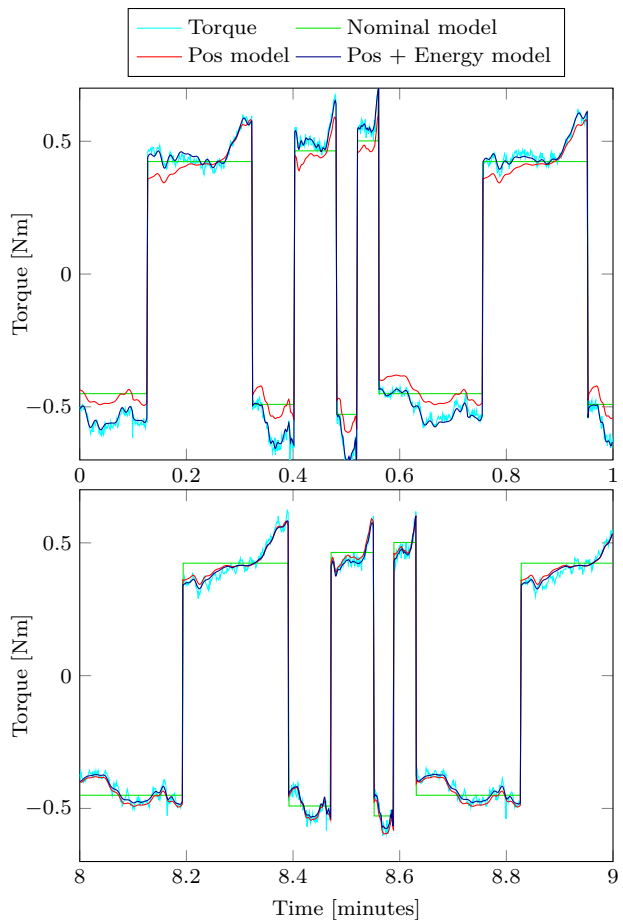

Fig. 9. Model fit to experimental data (YuMi). Upper plot shows an early stage of the experiment when the joint is cold. Lower plot a later stage, when the joint has been warmed up.

V. DISCUSSION

The proposed models try to increase the predictive power of common friction models by incorporating position- and temperature dependence. Systems with varying parameters can in theory be estimated with recursive algorithms, so called online identification. As elaborated on in Sec. I, online identification of friction models is often difficult in practice due to the presence of additional dynamics or external forces. The proposed methods are identified offline, during a controlled experiment, and are thus not subject to the problems associated with online identification. However, apart from the temperature related parameters, all suggested models are linear in the parameters, and could be updated recursively using for instance the well-known recursive least squares or Kalman filter algorithms [9].

Although outside the scope of this work, effects of joint load on the friction behavior can be significant [8]. Such dependencies could be incorporated in the proposed models using the same RBF approach as for the incorporation of position dependence, i.e. through an RBF expansion in the joint load ($l \in \mathcal{L}$) dimension according to $\phi(x) : (x \in \mathcal{P} \times \mathcal{E} \times \mathcal{L}) \rightarrow \mathbb{R}^{1 \times (K_p K_e K_l)}$, with K_l basis function centers along dimension $\mathcal{L}$. This strategy would capture possible position and temperature dependencies
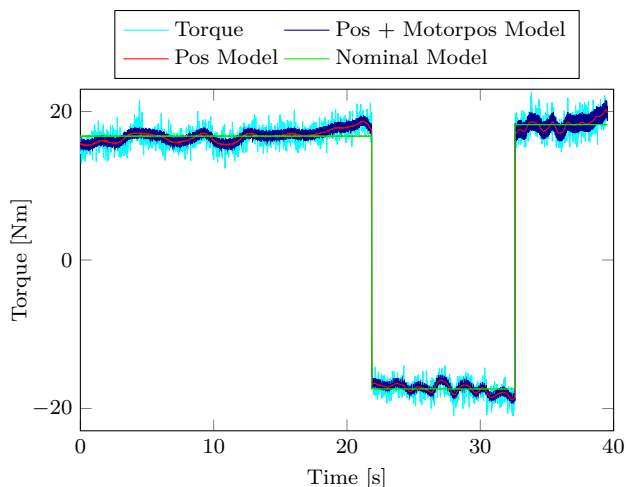
Fig. 10. Model fit including kernel expansion for motor position on IRB140. During $t = [0\,\mathrm{s}, 22\,\mathrm{s}]$, the joint traverses a full revolution of 2π rad. The same distance was traversed backwards with a higher velocity during $t = [22\,\mathrm{s}, 33\,\mathrm{s}]$. Notice the repeatable pattern as identified by the position dependent models.
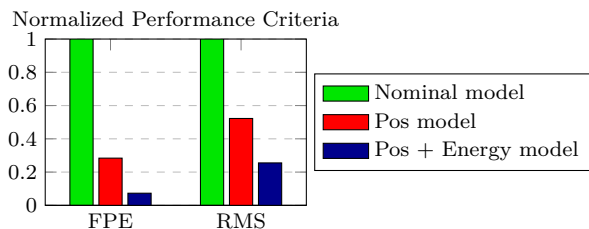

Fig. 11. Performance indicators for the identified models, YuMi.

in the load-friction interaction.

In its simplest form, the proposed energy dependent model assumes that the change in friction occurs in the Coulomb friction level. This is always valid for the Coulomb model, and a reasonable approximation for the viscous friction model if $k_c \gg k_v v$ or if the system is both operated and identified in a small interval of velocities. If the viscous friction $k_v v$ is large, the approximation will be worse. This suggests modeling the friction as

$$F_f = k_v(E)v + k_c(E)\,\mathrm{sign}\,(v) \qquad (27)$$

where the Coulomb- and viscous constants are seen as functions of the estimated energy signal E, i.e., a Linear Parameter-Varying model (LPV). To accomplish this, a kernel expansion including the estimated energy signal was suggested and evaluated experimentally.

Although models based on the internally generated power remove the need for temperature sensing in some scenarios, they do not cover significant variations in the
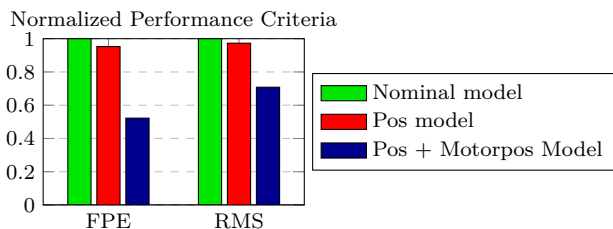

Fig. 12. Performance indicators for the identified models, IRB140.

surrounding temperature. The power generated in, for instance, an industrial robot is, however, often high enough to cause a much larger increase in temperature than the expected temperature variations of its surrounding [8].

VI. CONCLUSIONS

The modeling of both position and temperature dependence in systems with friction have been investigated. To model position varying friction, a Radial Basis Function network approach was adopted. It has been experimentally verified that taking position dependence into account can significantly reduce the model output error. It has also been reported that friction phenomena on both sides of a gearbox can be modeled using the proposed approach.

The influence of an increase in temperature due to power generated by friction has been modeled and estimated. The proposed approach was based on a first-order temperature input-output model where the power generated by friction was used as input. The model together with the proposed identification procedure was shown to capture the decrease in friction seen in an industrial robot during a long term experiment, this was accomplished without the need of temperature sensing.

REFERENCES

[1] H. Olsson, K. J. Åström, C. C. de Wit, M. Gäfvert, and P. Lischinsky, "Friction models and friction compensation," *European Journal of Control*, vol. 4, no. 3, pp. 176–195, 1998.

[2] P. Dahl, "A solid friction model," DTIC, Tech. Rep., 1968.

[3] C. C. De Wit, H. Olsson, K. J. Åström, and P. Lischinsky, "A new model for control of systems with friction," *Automatic Control, IEEE Trans. on*, vol. 40, no. 3, pp. 419–425, 1995.

[4] B. Armstrong-Hélouvry, P. Dupont, and C. C. De Wit, "A survey of models, analysis tools and compensation methods for the control of machines with friction," *Automatica*, vol. 30, no. 7, pp. 1083–1138, 1994.

[5] B. Armstrong, "Friction: Experimental determination, modeling and compensation," in *Robotics and Automation, Proc. 1988 IEEE Int. Conf. Pennsylvania*, 5 1988, pp. 1422–1427.

[6] P.-Y. Huang, Y.-Y. Chen, and M.-S. Chen, "Position-dependent friction compensation for ballscrew tables," in *Control Applications, 1998. Proc. 1998 IEEE Int. Conf., Trieste, Italy*, vol. 2, 9 1998, pp. 863–867.

[7] B. J. de Kruif and T. J. de Vries, "Support-vector-based least squares for learning non-linear dynamics," in *Decision and Control, 2002, Proc. IEEE Conf., Las Vegas*, vol. 2, 12 2002, pp. 1343–1348.

[8] A. C. Bittencourt and S. Gunnarsson, "Static friction in a robot joint - modeling and identification of load and temperature effects," *Journal of Dynamic Systems, Measurement, and Control*, vol. 134, no. 5, 2012.

[9] R. Johansson, *System modeling & identification*. Prentice-Hall, Englewood Cliffs, NJ, 1993.

[10] M. W. Spong, S. Hutchinson, and M. Vidyasagar, *Robot modeling and control*. Wiley, New York, 2006, vol. 3.

[11] G. H. Golub and C. F. Van Loan, *Matrix computations*. Johns Hopkins University Press, Baltimore, 2012, vol. 3.

[12] W. J. Rugh, *Linear system theory*. Prentice-Hall, Englewood Cliffs, NJ, 1996.

[13] K. P. Murphy, *Machine learning: a probabilistic perspective*. MIT press, Cambridge, Massachusetts, 2012.

[14] G. Bugmann, "Normalized gaussian radial basis function networks," *Neurocomputing*, vol. 20, no. 1âĂŞ3, pp. 97 – 110, 1998. [Online]. Available: http://www.sciencedirect.com/science/article/pii/S0925231298000277

[15] B. Wittenmark, K. J. Åström, and K.-E. Årzén, "Computer control: An overview," *IFAC Professional Brief*, 2002.